Spontaneous pattern formation upon incoherent waves: From modulation-instability to steady-state

Liad Levi,[1] Tal Schwartz,[1] Ofer Manela,[1]
Mordechai Segev[1] and Hrvoje Buljan[2]

[1]*Physics Department and Solid State Institute, Technion, Haifa 32000, Israel*
[2]*Physics Department, University of Zagreb, Zagreb, Croatia*
gsliadl@tx.technion.ac.il

Abstract: We study the long-range propagation of incoherent light following the modulation instability (MI) process in non-instantaneous nonlinear Kerr-type media. We find that the system eventually reaches a steady-state characterized by a lower degree of coherence than in the initial state, with small fluctuations around a pronounced mean value. We find that the average values of the spatial correlation distance at steady-state and the fluctuations around it, which are obtained either through ensemble averaging, or by spatial averaging, or via temporal averaging, are all identical. This feature may be viewed as indication of ergodic behavior, which occurs in the long-time evolution following incoherent MI. Finally, we find that the steady-state properties of the system depend on the initial coherence but not on the nonlinearity strength, although the system evolves faster to steady-state as the strength of the nonlinearity is increased.

©2008 Optical Society of America

References and links

1. M. C. Cross and P. C. Hohenberg, "Pattern formation outside of equilibrium," Rev. Mod. Phys. **65**, 851-1112 (1993).
2. V. I. Bespalov and V. I. Talanov, "Filamentary Structure of Light Beams in Nonlinear Liquids," Zh. Eksperim. i Teor. Fiz.-Pis'ma Redakt. **3**, 471 (1966); [translation: JETP Letters **3**, 307-312 (1966)].
3. M. D. Iturbe-Castillo, M. Torres-Cisneros, J. J. Sanchez-Mondragon, S. Chavez-Cerda, S. I. Stepanov, V. A. Vysloukh, and G. E. Torres-Cisnero*s*, "Experimental evidence of modulation instability in a photorefractive $Bi_{12}TiO_{20}$ crystal," Opt. Lett. **20**, 1853 (1995).
4. R. Malendevich, L. Jankovic, G. Stegeman, and J. Stewart Aitchison, *"*Spatial modulation instability in a Kerr slab waveguide," Opt. Lett. **26**, 1879-1881 (2001).
5. K. Tai, A. Hasegawa, and A. Tomita, "Observation of modulational instability in optical fibers," Phys. Rev. Lett. **56**, 135-138 (1986).
6. L. A. Lugiato, Chaos Solitons Fractals **4**, 1245-1251 (1994).
7. F. T. Arecchi, S. Boccaletti, and P. Ramazza, "Pattern formation and competition in nonlinear optics," Phys. Rep. **318**, 1-83 (1999).
8. R. W. Boyd, *Nonlinear Optics* (Academic Press, New York, 1994).
9. M. Mitchell, Z. Chen, M. Shih, and M. Segev, *"*Self-Trapping of Partially Spatially Incoherent Light," Phys. Rev. Lett. **77**, 490-493 (1996).
10. M. Mitchell and M. Segev, "Self-trapping of incoherent white light," Nature (London) **387**, 880-883 (1997).
11. M. Mitchell, M. Segev, T. H. Coskun, and D. N. Christodoulides, "Theory of Self-Trapped Spatially Incoherent Light Beams," Phys. Rev. Lett. **79**, 4990-4993 (1997).
12. M. Soljacic, M. Segev, T. Coskun, D. N. Christodoulides, and A. Vishwanath, "Modulation Instability of Incoherent Beams in Noninstantaneous Nonlinear Media," Phys. Rev. Lett. **84**, 467-470 (2000).
13. S. M. Sears, M. Soljačić, D. N. Christodoulides, and M. Segev, "Pattern formation via symmetry breaking in nonlinear weakly correlated systems," Phys. Rev. E **65**, 036620-9 (2002).
14. H. Buljan, A. Šiber, M. Soljačić, and M. Segev, "Propagation of incoherent "white" light and modulation instability in noninstantaneous nonlinear media," Phys. Rev. E **66**, 035601-4 (2002).

15. D. Kip, M. Soljacic, M. Segev, E. Eugenieva, and D. N. Christodoulides, "Modulation Instability and Pattern Formation in Spatially Incoherent Light Beams," Science **290**, 495-498 (2000).
16. D. Kip, M. Soljacic, M. Segev, S. M. Sears, and D. N. Christodoulides, "(1+1)-Dimensional modulation instability of spatially incoherent light," J. Opt. Soc. Am. B **19**, 502-512 (2002).
17. J. Klinger, H. Martin, and Z. Chen, "Experiments on induced modulational instability of an incoherent optical beam," Opt. Lett. **26**, 271-273 (2001).
18. T. Schwartz, T. Carmon, H. Buljan, and M. Segev, "Spontaneous Pattern Formation with Incoherent White Light," Phys. Rev. Lett. **93**, 223901-5 (2004).
19. Z. Chen, S. M. Sears, H. Martin, D. N. Christodoulides, and M. Segev, "Clustering of solitons in weakly correlated wavefronts," PNAS **99**, 5223-5227 (2002).
20. D. Anderson, L. Helczynski-Wolf, M. Lisak, and V. Semenov, "Features of modulational instability of partially coherent light: Importance of the incoherence spectrum," Phys. Rev. E **69**, 025601-025604 (2004).
21. D. Anderson, B. Hall, M. Lisak, and M. Marklund, "Statistical effects in the multistream model for quantum plasmas," Phys. Rev. E **65**, 046417-5 (2002).
22. E. Fermi, J. Pasta, and S. Ulam, "Studies of non linear problems," Los Alamos Rpt. LA-1940 (1955).
23. A. Picozzi, "Towards a nonequilibrium thermodynamic description of incoherent nonlinear optics," Opt. Express **15**, 9063-9083 (2007).
24. S. Pitois, S. Lagrange, H. R. Jauslin, and A. Picozzi, "Velocity Locking of Incoherent Nonlinear Wave Packets," Phys. Rev. Lett. **97**, 033902-5 (2006).
25. S. Dyachenko, A. C. Newell, A. Pushkarev, and V. E. Zakharo., "Optical turbulence: weak turbulence, condensates and collapsing filaments in the nonlinear," Physica D (Amsterdam) **57**, 96-160 (1992).
26. E. A. Kuznetsov, A. V. Mikhailov, and I. A. Shimokhin, "Nonlinear interaction of solitons and radiation," Physica D **87**, 201-215 (1995)
27. The only exception we know of is M. Rigol *et al.*, Phys. Rev. Lett. **98**, 050405-5 (2007) where a quantum integrable system relaxes to a steady state, carrying memory of initial conditions.
28. D. N. Christodoulides, E. D. Eugenieva, T. H. Coskun, and M. Segev, "Equivalence of three approaches describing partially incoherent wave propagation in inertial nonlinear media," Phys. Rev. E **63**, 035601-035603 (R) (2001).
29. L. Mandel and E. Wolf, *Optical Coherence and Quantum Optics*, (Cambridge University Press, 1995).
30. E. T. Jaynes, "Information Theory and Statistical Mechanics," Phys. Rev. **106**, 620-630 (1957).
31. E. T. Jaynes, "Information Theory and Statistical Mechanics. II," Phys. Rev. **108**, 171-190 (1957).
32. V.G. Makhan'kov and O. K. Pashaev, "Nonlinear Schrödinger equation with noncompact isogroup," Teor. Mat. Fiz. **53**, 55 (1982) [Theor. Math. Phys. **53**, 979-987 (1982)].
33. M. Soljačić, K. Steiglitz, S. M. Sears, M. Segev, M. H. Jakubowski, and R. Squie, "Collisions of Two Solitons in an Arbitrary Number of Coupled Nonlinear Schrödinger Equations," Phys. Rev. Lett. **90**, 254102-254105 (2003).
34. H. Buljan, M. Segev, and A. Vardi, "Incoherent Matter-Wave Solitons and Pairing Instability in an Attractively Interacting Bose-Einstein Condensate," Phys. Rev. Lett. **95**, 180401-4 (2005).

1. Introduction

The phenomena of spontaneous pattern formation and modulation instability (MI) are found in many nonlinear systems in nature [1]. In such a process, an extended state breaks up, disintegrating into localized excitations (e.g., filaments in spatial optical systems [2-4] or short pulses in temporal ones [5]), as random noise gets amplified through nonlinear evolution. The end result could be an ordered pattern (typically, if the system supports stable solitons) [5], or an ongoing dynamic process such as catastrophic collapse [2] or even chaos [6,7]. In spatial optical systems, MI was traditionally believed to be a fully coherent process [8]. However, following the discovery of incoherent (random-phase) solitons [9-11], MI was predicted [12-14] and demonstrated [15-19] also in incoherent wave systems. These studies revealed that incoherent MI occurs only when the nonlinearity exceeds a well-defined threshold value, which manifests the balance point between two opposing tendencies: the nonlinear self-focusing of small perturbations, and their linear diffusive washout resulting from the combined effect of diffraction and incoherence [12-16]. Below the threshold, no pattern emerges, whereas above threshold self-focusing leads to the formation of a periodic pattern [12-21]. The studies on incoherent MI were thus far concerned only with the early stages of MI formation. It is, however, natural to ask what happens after the MI pattern has already formed, and continues to evolve for a long distance. Does the system ever relax to a steady-state? If so, how is this steady-state characterized, and how does it depend on the initial state of coherence and the strength of the nonlinearity?

The fundamental question of relaxation to equilibrium via nonlinearity dates back to Fermi, Pasta and Ulam [22]. Several recent studies address relaxation in the context of incoherent light ([23,24] and references therein). In those systems, relaxation processes were studied by using kinetic wave theory [23-25], in which linear dispersive effects dominate over the nonlinear phenomena [23]. It is generally accepted that relaxation occurs in non-integrable systems, where diffusion in phase space leads to equilibrium [23,24], whereas integrable systems are expected to exhibit recurrent motion reflecting the regular phase space structure of nested tori [23]. Despite that general trend, one may find examples of relaxation in integrable systems [26,27].

Here, we study the long-range propagation of incoherent waves, following incoherent MI, in non-instantaneous Kerr-type media, and in one spatial dimension. In section 2 we describe the mathematical model we utilize, and in section 3 we define the physical quantities describing the relaxation process in the system. In the following section (4) we will show that this integrable classical nonlinear wave system reaches a steady-state (a dynamic equilibrium state), at which the coherence is smaller than the initial coherence, i.e., the disorder within the beam increases to its steady-state value. In section 5 & 6 we show that the average values of the spatial correlation distance at steady-state and the fluctuations around it, obtained either through ensemble averaging, or by spatial averaging, or via temporal averaging, are all identical. This feature may be viewed as an indication that the system is ergodic. In section 7, we show that, above the MI threshold, the spatial correlation distance at the steady-state does not depend on the nonlinearity strength, but on the initial coherence; however, the strength of the nonlinearity scales the distance to equilibrium. Finally, we summarize our results in section 8.

2. Model

We study the propagation of quasi-monochromatic spatially incoherent light in a non-instantaneous Kerr medium by using the *modal theory* [11]. The slowly-varying envelope of the partially-incoherent wave $E(x,z,t)$ is represented via the sum of orthonormal modes $\Psi_n(x,z)$, as $E(x,z,t) = \sum_n c_n(t)\,\Psi_n(x,z)$, where the modal coefficients c_n stochastically fluctuate in time in a fully uncorrelated fashion, that is, $\left\langle c_m c_n^* \right\rangle = \delta_{mn} d_n$ [11]; d_n are real numbers representing the modal weights. The modal functions $\Psi_n(x,z)$, within the slowly-varying amplitude approximation, obey a set of coupled nonlinear-Schrödinger equations (also known as the integrable N-Manakov set [29-30]),

$$i\frac{\partial \Psi_n(x,z)}{\partial z} + \frac{\partial^2 \Psi_n(x,z)}{\partial x^2} + I(x,z)\Psi_n(x,z) = 0 \quad n=1,2....N, \tag{1}$$

where $I(x,z) = \sum_n d_n \left|\Psi_n(x,z)\right|^2$ denotes the time-averaged intensity (units are dimensionless as in [31]); the average is taken with respect to the response time of the nonlinearity, which is considerably longer than the fluctuation time of the modal coefficients $c_n(t)$. The system can be equivalently described by the mutual coherence function

$$B(x_1,x_2,z) = \left\langle E^*(x_2,z,t)E(x_1,z,t) \right\rangle = \sum_n d_n \Psi_n(x_1,z)\Psi_n^*(x_2,z) \tag{2}$$

describing the field correlations between two spatially-separated points across the wave [28]. The evolution of the mutual coherence function $B(x_1,x_2,z)$ can be derived straightforwardly from Eq. (1):

$$\frac{\partial B(x_1,x_2,z)}{\partial z} = i\left(\frac{\partial^2 B(x_1,x_2,z)}{\partial x_1^2} - \frac{\partial^2 B(x_1,x_2,z)}{\partial x_2^2}\right) + i\big(B(x_1,x_1,z) - B(x_2,x_2,z)\big)B(x_1,x_2,z) \quad (3)$$

One of the integrals of motion of this system, that we will utilize later on, is $\iint |B(x_1,x_2,z)|^2 dx_1 dx_2$. This follows after integrating Eq. (3) over x_1 and x_2, and by assuming that the fields decay to zero at infinity (which is reasonable for physical systems), or that the boundary conditions are periodic (as we assume in this paper).

3. Physical quantities used for describing relaxation

The state of the system is fully described with the mutual coherence function $B(x_1,x_2,z)$ (or equivalently the modes $\Psi_n(x,z)$, and their weights d_n). We emphasize that the initial condition for incoherent MI is $B(x_1,x_2,z=0) = B_0(x_1-x_2) + B_1(x_1,x_2,z=0)$, where B_0 denotes a beam with uniform intensity $B_0(0) \equiv B(x,x) = I(x) \equiv I_0$, while $B_1(x_1,x_2,0)$ denotes small initial noise upon the beam [12-16]. Thus, at a given propagation distance ("time") z, the mutual coherence function and local physical quantities derived from it (such as the intensity pattern emerging from the MI process) depend on the spatial variable(s) and on the particular realization of the initial noise. It is however desirable that the quantities characterizing the long-term evolution do not depend on the particular realization of the noise. Hence, it is essential to repeat the simulations many times, each time with a different structure of the initial noise (of the same statistics), and obtain ensemble-averaged values. In order to understand the long-term dynamics, following incoherent MI, it is essential to study certain averages made over $B(x_1,x_2,z)$. We introduce the spatial average $\langle\cdots\rangle_x = \frac{1}{2d}\int_{-d}^{d}\cdots dx$ ($2d$ is the size of the numerical window), the "time average" (which actually should be defined as "propagation averages") $\langle\cdots\rangle_z$ (averages over the propagation coordinate), and the ensemble average $\langle\cdots\rangle_e$ (in a similar fashion, statistical mechanics does not consider exact positions and velocities of molecules in a gas, but rather distributions and averaged quantities). All possible realizations of the initial noise span the ensemble. The ensemble averages are obtained by repeating numerical simulations, each time with a different realization of the (random) initial noise, and averaging a quantity over the thus obtained ensemble. As we show below, we find a relation between these averages, calculated in fundamentally different fashions. We also study the fluctuations around these averages which are quantified by the standard deviations (and higher moments).

The physical quantities utilized to describe relaxation are as follows. The first is the normalized transverse spatial correlation distance

$$l_c(x,z) = \left\langle |\mu(x,x',z)|^2 \right\rangle_{x'} = \frac{1}{2d}\int_{-d}^{d} |\mu(x,x',z)|^2 \, dx' \quad (4)$$

Here, $\mu(x_1,x_2,z) = B(x_1,x_2,z)/\sqrt{I(x_1,z)I(x_2,z)}$ [29] is the complex coherence factor, for which $0 \le |\mu(x_1,x_2,z)| \le 1$. In the limiting case the fields at x_1 and x_2 are completely uncorrelated (fully correlated), $|\mu(x_1,x_2,z)| = 0$ ($|\mu(x_1,x_2,z)| = 1$, respectively). The quantity $l_c(x,z)$ is a measure for the order/disorder of the beam, as it is directly related to the randomness of the propagating field [29] [$l_c(x,z) = 1$ for full coherence between all points on the cross section and point x, whereas $l_c(x,z) = 0$ for full incoherence]. Besides $l_c(x,z)$, we analyze the

evolution of its ensemble average $\langle l_c(x,z)\rangle_e$, spatial average $\langle l_c(x,z)\rangle_x = L_c(z) = \dfrac{1}{2d}\int l_c(x,z)dx$,

and "time" $\langle \cdots \rangle_z$ average. The quantity $L_c(z)$ describes the average spatial correlation distance at a given plane z.

Next quantity of interest is the transverse-variance of the intensity

$$M(z) = \left\langle \left(I(x,z) - \bar{I}(z)\right)^2 \right\rangle_x = \frac{1}{2d}\int_{-d}^{d}\left(I(x,z) - \bar{I}(z)\right)^2 dx \tag{5}$$

where $\bar{I}(z) = \langle I(x,z)\rangle_x = I_0$ (conservation of power). $M(z)$ is a measure of the modulation depth (visibility) of the emerging pattern following MI at a plane located at z. This quantity is particularly useful as it is connected to the nonlinear (potential U) and diffractive (kinetic T) energies of the beam. Namely, the Hamiltonian of the system

$$H = \frac{1}{2d}\int_{-d}^{d}dx\left[\sum_i\left|\frac{\partial\psi_i(x,z)}{\partial x}\right|^2 - I(x,z)^2\right] \equiv T(z) + U(z) \tag{6}$$

is conserved. The intensity variance may be written as

$$M(z) = \frac{1}{2d}\int_{-d}^{d}dx\left[I(x,z)^2 - \bar{I}(z)^2\right] = -U(z) - I_0^2 = -H - I_0^2 + T(z) \tag{7}$$

Clearly, if $M(z)$ reaches steady-state, so do the nonlinear (potential) and diffractive (kinetic) "energies" within the beam.

Finally, we will use the spatial power spectrum of the incoherent beam to study relaxation. This quantity is the incoherent sum of the Fourier transforms of the N modes comprising the beam, that is, $P(k_x,z) = \sum_n d_n\left|\int dx e^{-ik_x x}\psi_n(x,z)\right|^2$.

4. Results: Dynamics of averaged values

In what follows we simulate the evolution of the beam numerically over very large propagation distances (by solving Eq. (1) with a standard split-step Fourier method), and study the evolution of quantities defined in Sec. 3. The simulation consists of launching $N=3$ uncorrelated plane waves into the system, $\psi_n(x,0) = e^{ik_n x} + \delta\psi_n$ $n = 1,2,3$, where $\delta\psi_n$ denotes small initial noise upon each mode (see Fig. 1(a)); for all our initial conditions $\left|\delta\psi_n/\psi_n\right| < 5\%$. The modal weights d_n are chosen to conform to a Gaussian distribution in k_x space (see Fig. 1(b)). This means that the incoherent beam comprises of several plane waves (each superimposed with small noise) propagating at symmetrical angles around the optical axis z, while the ratios among the amplitudes are given by the set $\{d_n\}$. The noise is chosen so that its spectral density is a Gaussian which is significantly wider than the Gaussian modal distribution of the beam, depicted in Fig 1(b).
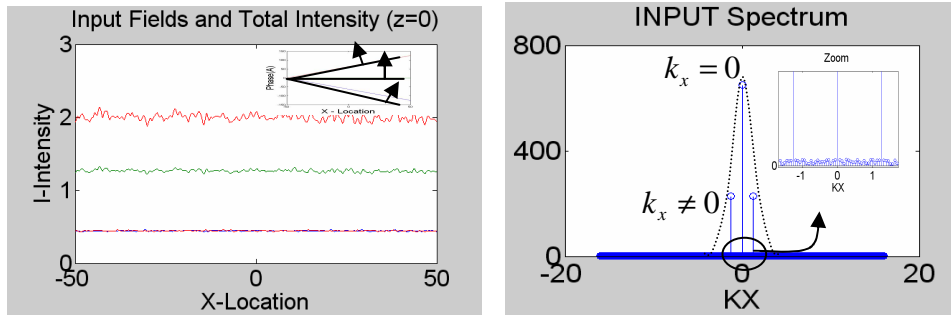
Fig. 1. (a) Input field distribution $E(x,z=0)$ and the total intensity at the input $(z=0)$. The insert shows the linear phase upon all three plane waves, indicating that the modes propagate in different directions with respect to the z-axis (direction of the central plane wave). The fluctuations in all three field amplitudes reflect one particular realization of the input noise. (b) Spatial power spectrum of the input field $(z=0)$. The power within the three plane waves conforms to a Gaussian distribution in k_x-space. The insert zooms to show the presence of small initial noise in all spatial wave vectors.

The dynamics of the intensity $I(x,z)$, $l_c(x,z)$ and $M(z)$, for a single-shot propagation is depicted in Fig. 2(a), 2(b), and 2(c), respectively. From these figures we get an impression that the system evolves into some kind of steady-state. Note that $I(x,z)$ and $l_c(x,z)$ are local quantities in the sense that they depend on both x and z and their values at given coordinates depend on the structure of the initial noise (in contrast, $M(z)$ is already averaged over the spatial variables).
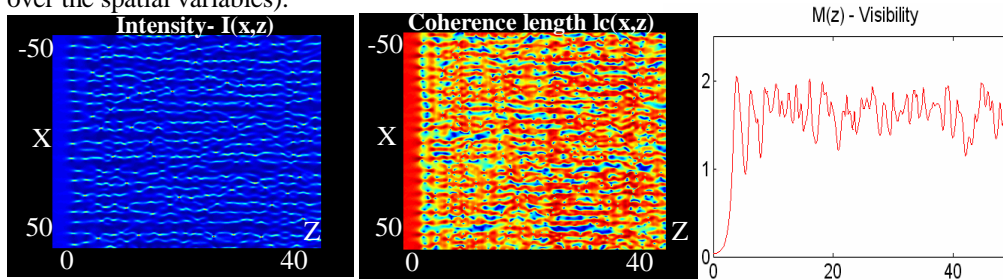

Fig. 2. (a) Emergence and dynamics of the incoherent MI intensity pattern, as the system evolves towards steady-state. (b) Evolution of the transverse correlation distance upon the partially-spatially-incoherent beam, as the system evolves towards the steady state. (c) Evolution of the transverse intensity-variance, $M(z)$, which is a measure for the modulation depth (visibility) of the evolving MI pattern shown in Fig. 2(a).

In order to quantify the relaxation to the steady-state (which is some kind of equilibrium), and obtain results which are independent of the particular structure of the initial noise, we study the dynamics of the ensemble and the x-averaged spatial correlation distance, illustrated in Fig. 3. Figure 3(a) shows a contour plot of the ensemble-averaged value of $\left\langle l_c(x,z)\right\rangle_{e=800}$, for average taken over 800 realizations of the initial noise. The simulations are similar to those of Fig. 2(b), but are carried out for longer propagation distances, and are averaged over the ensemble. We clearly see that the ensemble-averaged value $\left\langle l_c(x,z)\right\rangle_{e=800}$ is x-independent. This is underpinned in Figs. 3(b) and 3(c), which are cross sections of Fig. 3(a) taken at different arbitrary x values. The result that $\left\langle l_c(x,z)\right\rangle_{e=800}$ is x-independent follows from the fact the initial condition without the noise has translational symmetry. While small

noise breaks this symmetry via MI, the average over the noise-ensemble restores this symmetry because the noise-ensemble should have no preferential x point. This result motivates us to explore and compare the ensemble-averaged $\langle ... \rangle_e$ and the spatially-averaged $\langle ... \rangle_x$ values of the correlation distance.
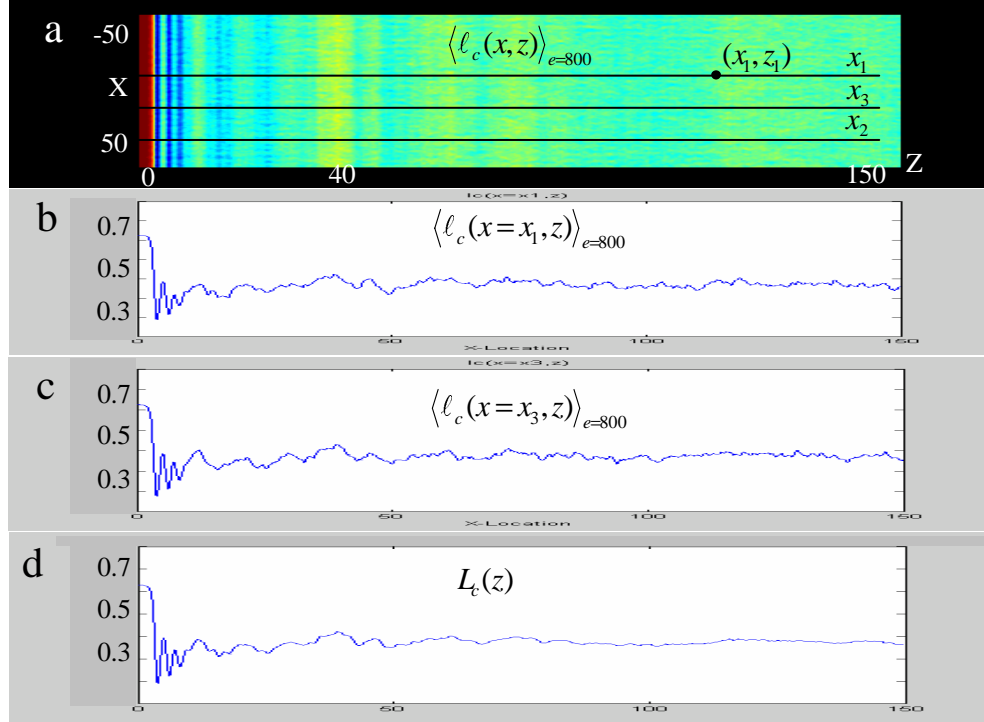

Fig. 3. (a) Ensemble-averaged value of $\langle l_c(x,z) \rangle_{e=800}$ taken over 800 realizations of the initial noise The initial transient behavior for $z < 40$, and the final steady-state are clearly observed. (b),(c) Dynamics of $l_c(x,z)$ along to arbitrary chosen x values, showing that the behavior in equilibrium is x-independent. (d) Dynamics of $L_c(z)$ shows the same behavior as in (b) and (c). See text for details.

Figure 3(d) shows evolution of the $L_c(z) = \langle l_c(x,z) \rangle_x$. We observe that it is essentially identical to the evolution of $\langle ... \rangle_e$, from which we conclude that in this system, an average (of some local quantity) over the noise-spanned ensemble, is identical to the average over the spatial variable. This relation may be viewed as ergodic behavior. We should mention that in our numerical simulations $L_c(z)$ can depend upon the finite system size (numerical window) used in our simulations, while ensemble averaging depends on the size of the numerically used ensemble. It is clear that, when the system size is $2d$ and ensemble size become infinite, the two quantities are expected to be identical.

The most important result that follows from the simulations depicted in Fig. 3 is that, after incoherent MI has occurred, the system evolves into a steady state, for which the final spatial correlation distance is smaller than the initial one. We note that, before reaching the steady-state, the system goes through an oscillatory transient period where $L_c(z)$ fluctuates, and then it gradually relaxes to a steady-state (see Fig. 3(d)). A similar behavior is observed

for $M(z)$ (see Fig. 2(c)), although it is opposite in its nature: while the system relaxes to its lower degree of coherence in steady-state, its visibility is increasing. This suggests that the two quantities, $L_c(z)$ and $M(z)$, are connected.

Figure 4 shows medium-range simulations of, $L_c(z)$ (solid line; left axis) and $M(z)$ (dashed line; right axis) superimposed on the picture of the MI intensity pattern. Figure 4 reveals that $L_c(z)$ and $M(z)$ exhibit anti-correlated oscillations throughout propagation.
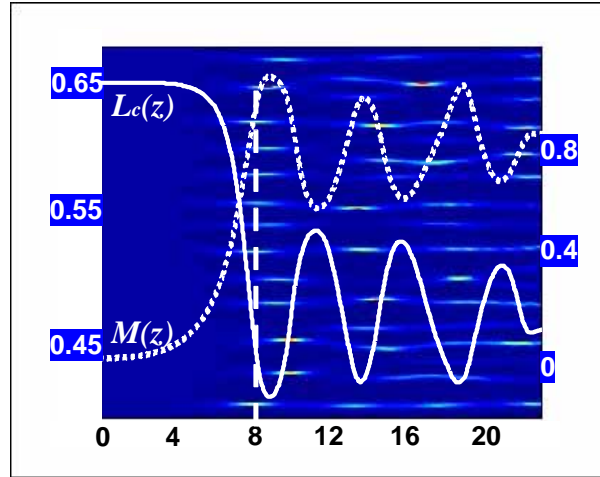

Fig. 4. Emergence and dynamics of the incoherent MI pattern as the system evolves towards equilibrium. The intensity pattern is shown in the background, while superimposed on it are the average correlation distance $L_c(z)$ (solid line; left axis), and the transverse-variance of the intensity, $M(z)$ (dashed line; right axis).

We explain this observation by employing the conservation laws of our integrable system. If the beam maintains a uniform intensity during propagation, $I(x,z) \cong I_0$, then the definition of $L_c(z)$, and the fact that $\int |B(x_1, x_2, z)|^2 dx_1 dx_2$ is an integral of motion, yield that the average spatial-correlation-distance does not change during propagation, $L_c(z) \cong \frac{1}{2dI_0^2} \int |B(x_1, x_2, z)|^2 dx_1 dx_2 = const.$ This situation, which necessitates a uniform intensity (or almost uniform), can occur (i) in the early stages of propagation, when the MI pattern has not formed yet (e.g., Fig. 4 for $z \leq 3$), and (ii) when the nonlinearity is below the MI threshold (the pattern never develops) [12-19]. However, Fig. 4 reveals much more: that $L_c(z)$ and $M(z)$ are anti-correlated not only in the regimes where the intensity is uniform, but actually throughout evolution, including at stages where the beam has high-contrast structures within it (see, for example, the intensity pattern in Fig. 4 at planes $z = 9,13,18$). To explain this, we employ Eq. (7), and the expression for the kinetic term via the spatial power spectrum of the light $T = \int dk_x k_x^2 P(k_x, z)$. When a high-contrast pattern appears, $M(z)$ increases; thus, according to Eq. (3), T increases, and the power spectrum $P(k_x, z)$ broadens. At the same time, the increase in the width of the power spectrum $P(k_x, z)$ is generally associated with a decrease in the spatial correlation distance $L_c(z)$ (see Chap. 5 in

[29]). This explains why $M(z)$ and $L_c(z)$ are always anti-correlated. An alternative, more intuitive, explanation is as follows. When the pattern is of high contrast ($M(z)$ is large), regions of high intensity occupy a smaller region in space (conservation of power), i.e., the beam is effectively squeezed. Squeezing the beam in space due to high-contrast intensity fluctuations reduces the spatial coherence (just as the spatial coherence increases when an incoherent beam experiences diffraction-broadening [29]). We find this anti-correlation effect in all our simulations on incoherent MI, irrespective of the number of fields comprising the incoherent beam and of all parameters involved.

In this section we have shown that our system, described by a classical integrable model, enters a steady-state after long term propagation. Let us discuss the differences between our findings and another example of relaxation in an integrable system. It is well known that a localized excitation of coherent light [described with the NLSE] can relax to a soliton state by emitting redundant radiation to infinity (e.g., see [26]). This scenario is closely related to the fact that an integrable system is naturally divided into two subsystems: one of which includes one localized state (the soliton), whereas the other subsystem includes non-localized modes (radiation modes), which play the role of a dissipative-like mechanism enabling relaxation. In contrast to that scenario, where the separation between localized and extended states is clear-cut [26], our system of incoherent MI, albeit being integrable - cannot be easily separated into two such subsystems (simply because it is difficult to identify the soliton states – including the high-order ones – embedded within the pattern emerging from the incoherent MI process). Consequently, the dynamic equilibrium state described here is fundamentally different from that of Ref. [26].

5. Fluctuations around the mean values

In order to characterize the steady-state features of a many-body system, the mean values are insufficient. We would like to address the following questions. What are the fluctuations around the mean values? What is the probability of measuring $l_c(x, z)$ within some interval $l_c \pm \Delta l_c$, after the system has reached steady-state? In addition, it is very interesting to know whether propagation in z spans the same statistics as the ensemble does. In order to address these questions, we take a single coordinate (x_1, z_1), where z_1 is sufficiently large so that the system has already reached steady-state, and calculate the distribution of the $l_c(x_1, z_1)$ values that result from all possible values of initial-noise (i.e., these values are obtained by repeating the simulation many times, each time with different initial noise, and calculating $l_c(x_1, z_1)$). This distribution is plotted in Fig. 5(a). Figure 5(b) shows the distribution of the $l_c(x, z)$ values calculated at a fixed $x = x_1$, as it evolves in z [only $z > 40$ values were taken into account, to ensure that in all cases the system has reached steady-state]. When the two histograms are normalized to have unity area, they serve as valid probability measures from which we can calculate fluctuations around the mean physical values. For example, in both histograms, the STD is 25% of the mean. Thus, fluctuations around the averaged value $\langle l_c(x, z) \rangle_e$ are fairly large (25%).

It is important to point out that both probability distributions appear to be equal. This may be quantitatively inferred as follows. We calculate the moments for both histograms, up to the 4th moments and compare them. Comparison between the moments of the two histograms reveals a high correspondence between their values. For example, the mean (1st moment) exhibit 98% correspondence, the STD (2nd moment) exhibits 96% correspondence and the 3rd and 4th moments exhibits 83% and 78% correspondence, respectively. We believe that the decrease in correspondences between the ensemble histogram (Fig. 5(a)) and cross-sectional histogram (Fig. 5(b)) as we go to higher moments is because the higher moments require a

larger statistics. That is, for accurate higher moments we need a much larger ensemble and a much longer evolution in z in order to sample the whole "phase space" of the system.

These findings suggest that both histograms display the same statistics. This can be viewed as another ergodic behavior of the system in the sense that probabilities obtained by ensemble averaging, or averaging over ("time") z-coordinate (also x-coordinate, see Sec 4.), are practically identical.
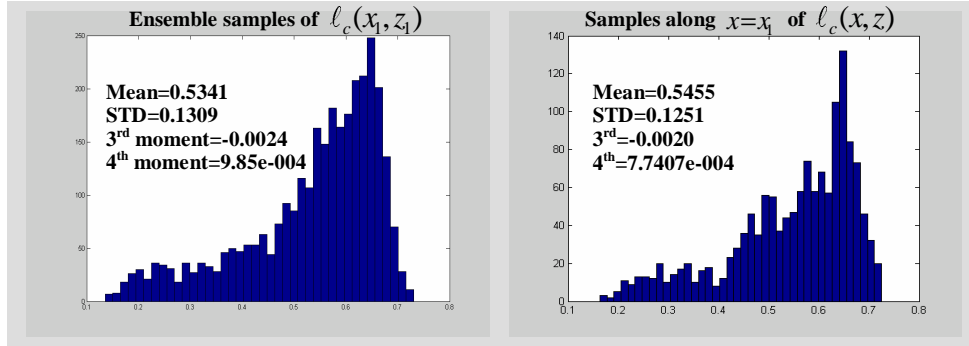

Fig. 5. (a) Distribution of the l_c values at the point (x_1, z_1) shown in Fig. 3a, from an ensemble of 800 samples. (b) Distribution of the $l_c(x,z)$ values chosen from a cut taken at a fixed $x = x_1$, and for various z. The values are chosen from a single-shot evolution, after the system has reached steady-state (i.e., only values for $z > 40$ taken).

6. Evolution of the spatial power spectrum

Another interesting and useful indication for the dynamics of the system is provided by analyzing the power spectrum of the incoherent beam as it propagates (see Fig. 6). Figure 6(a) shows the contour plot of the spatial power spectrum for a beam comprised of 41 plane waves, with modal weights - d_n - chosen at the input (z=0) to conform to a Gaussian distribution in k_x space (Fig. 6(b)). Figure 6(c) shows the power spectrum at z=150. Evidently, the power spectrum significantly broadens until reaching a given width, at which it stabilizes. This initial increase in width is consistent with the decrease of the spatial correlation distance (see Sec 4). To show this feature more quantitatively, Fig. 6(d) displays cross-sections of Fig. 6(a) at various propagation distances.

We should emphasize that the steady-state reached in the system is not a thermodynamic equilibrium, where the modes of the linear system (plane waves) would have been populated according to the Boltzmann distribution. This is in fact an expected result, because Eq. (1) possesses an infinite number of integrals of motion (conserved quantities; not only energy is conserved), thus the dynamics is far more restrictive in phase space. We conjecture that the properties of our dynamic steady-state are governed by the maximal entropy principle, constrained by the integrals of motion in the sense of Refs. [30,31].
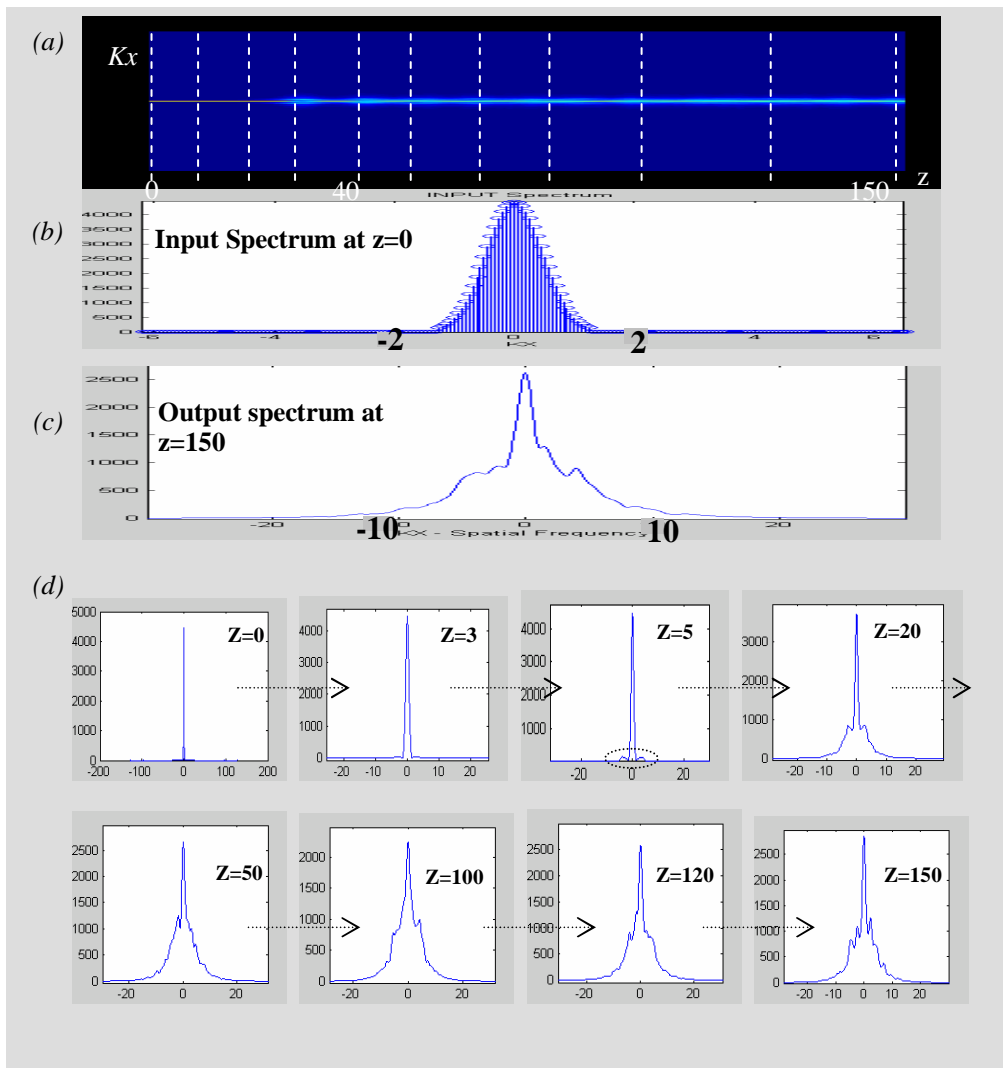
(a) Kx

0   40   INPUT Spectrum   150   z

(b) **Input Spectrum at z=0**

-2   Kx   2

(c) **Output spectrum at z=150**

-20   -10   Kx - Spatial Frequency   10   20

(d)

Z=0   Z=3   Z=5   Z=20

Z=50   Z=100   Z=120   Z=150

Fig. 6. (a) Evolution of the power spectrum along z. (b) Input power spectrum. (c) Power spectrum at $z = 150$. (d) Power spectrum at various propagation distances. At $z = 5$, the side-lobes are significant, indicating MI formation. For $z > 5$, the power spectrum broadens gradually, until it reaches a constant width and fluctuates around that value, indicating the existence of a steady-state.

7. Dependence on the nonlinearity and on the degree of coherence

We now study how the steady-state depends on the strength of the nonlinearity. Our system is Kerr-type, where the nonlinear index-change is proportional to the intensity, hence the system dependence on the nonlinearity strength is equivalent to its dependence on the optical intensity. Figure 7(a) shows the evolution of the average spatial correlation distance $L_c(z) = \langle l_c(x, z) \rangle_x$ for different values of the initial intensity (all cases are above the MI threshold). For all values of the intensity (i.e., nonlinearity), the initial coherence $L_c(z = 0)$ is the same. After the system has reached a steady state, $L_c(z)$ seems to fluctuate around the same average value for all values of the nonlinearity. In order to quantify this, we rely on our

previous results $\langle l_c(x,y)\rangle_e = \langle l_c(x,y)\rangle_x = \langle l_c(x,y)\rangle_z$, and employ an averaging window, which moves along z [see Fig. 7(a)]; we calculate the average and the STD of $L_c(z)$ within that window as function of its position. This quantifies the difference/similarity in the evolution of $L_c(z)$ for different levels of the nonlinearity. The length of the window Δz is chosen to be much longer than the mean period of the fluctuations in $L_c(z)$, but much shorter than the period of the large oscillations $L_c(z)$ exhibits during the initial stages (see Figs. 3 and 4). The use of this window is fully equivalent to averaging $l_c(x,z)$ over a rectangle in the (x,z) plane which extends for a length of $2d$ in the x-direction, and Δz in the z-direction.
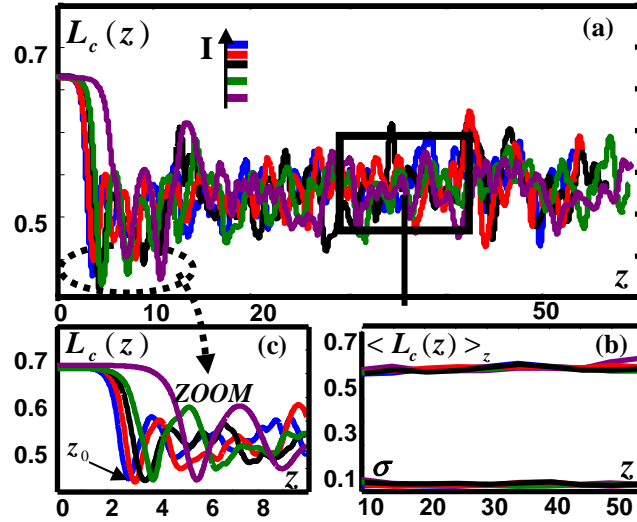

Fig. 7. (a) Evolution of the correlation distance, $L_c(z)$, for five values of the initial intensity; the plots are similar for $z \geq 10$. (b) $\langle L_c(z)\rangle_z$ and the STD σ_z. Both are independent of the position of the center of the averaging window. (c) Zooming into the initial stages of evolution; the distance to equilibrium, increases as the total intensity decreases.

We clearly observe that $\langle L_c(z)\rangle_z$ and the STD σ_z are practically the same in all simulations [Fig. 7(b)]. That is, the nonlinearity has a negligible influence on the correlation properties at the steady-state. This observation is intriguing: for intensity values below MI threshold, $L_c(z)$ remains constant, maintaining its initial value $L_c(z=0)$, whereas for intensity values above the MI threshold (e.g., those of Fig. 7), $L_c(z)$ clearly evolves, yet its steady-state value $\langle L_c(z)\rangle_z$ does not depend on intensity, as long as it is above the MI threshold. This implies that the steady-state value $\langle L_c(z)\rangle_z$ exhibits a sharp decrease when the nonlinearity goes through the MI threshold. This is a surprising observation, because the system is Kerr-type, hence it is tempting to think that the evolution dynamics is scalable. Evidently, the sharp transition in $\langle L_c(z)\rangle_z$, when the nonlinearity goes through the MI threshold, defies scalability. Rather, the sharp transition is indicative of a phase-transition between two generically different behaviors [12-14]. What is indeed scalable is the distance

("time") to reach equilibrium, which is inversely proportional to the strength of the nonlinearity, as we find from many simulations as those displayed in Fig. 7(c).

Finally, we study the dependence of the steady-state properties on the initial coherence of the system, $L_c(z=0)$. We do this by varying the ratio between the modal weights $\{d_n\}$, while keeping the initial total intensity ($\sum_n d_n$) unchanged. Figure 8 shows the relative loss of spatial coherence of the beam at the steady-state, $\Delta L_c / L_c(z=0)$ [left axis; black curve, where $\Delta L_c = L_c(z=0) - \langle L_c(z) \rangle_z$], as a function of the initial coherence, $L_c(z=0)$. Figure 8 also shows the ratio $\sigma_z / \langle L_c(z) \rangle_z$ (right axis; red curve), which indicates the magnitude of the fluctuations at the steady-state, also as a function of $L_c(z=0)$. We find that the largest relative loss of coherence and the largest fluctuations occur at similar values of the initial coherence $L_c(z=0)$. The existence of both maxima observed in Fig. 8 can be understood by considering the two extreme cases of fully-coherent light and highly-incoherent light, where $\Delta L_c / L_c(z=0) = 0$ and $\sigma_z / \langle L_c(z) \rangle_z = 0$. For a fully coherent beam, MI occurs without any threshold, and always remains coherent ($L_c = 1$ for all z). For a highly incoherent beam, such that it is below the MI threshold, L_c remains unchanged for all z, because $M(z) = 0$ (see discussion above). Between these two extreme cases, the coherence of the system at steady-state is smaller than the initial coherence, hence a maximum change in coherence and in STD must occur at some intermediate value of $L_c(z=0)$. Thus, as Fig. 8 reveals, the initial level of coherence $L_c(z=0)$ strongly affects the steady-state of the system.
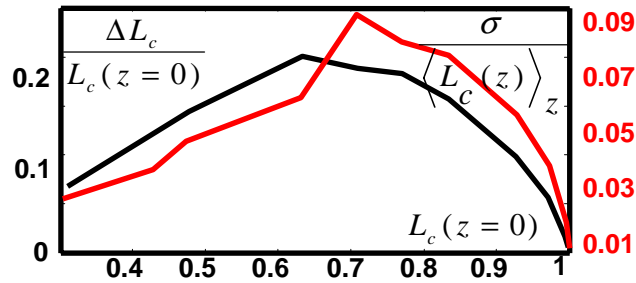

Fig.8. Relative loss of coherence $\Delta L_c / L_c(z=0)$ (black curve), and the ratio $\sigma_z / \langle L_c(z) \rangle_z$ (red curve) at steady-state, both as functions of the initial coherence.

8. Conclusion

Summarizing our findings, we conclude first that the long-range propagation of incoherent light following the modulation instability (MI) process in non-instantaneous nonlinear Kerr-type brings the system into a steady-state. We have shown that the experimentally-relevant quantities (spatial correlation distance and intensity-variance) after long-term propagation converge to mean values with fluctuations around them. The steady-state coherence is found to be lower than in the initial coherence. Further, we have also shown that the averages of the spatial correlation distance obey $\langle ... \rangle_e = \langle ... \rangle_x = \langle ... \rangle_z$, and that their STD's obeys $\sigma_e = \sigma_x = \sigma_z$. This can be viewed as ergodic behavior. We have found that the mean value of coherence at the steady state depends on the initial coherence of the system, but not on the strength of the nonlinearity (above the MI threshold).

Our results are interesting also from the point of view of integrability. The numerical simulations are performed in a classical nonlinear integrable system (the N-Manakov system with periodic boundary conditions), where it was generally believed that dynamics cannot relax but rather exhibit recurrences. Clearly, our system does reach a steady-state, with no recurrence.

We expect that the long-term evolution following incoherent MI in other systems will exhibit relaxation to some kind of steady-state as well. We believe that our findings in optics have counterpart in other fields, such as matter waves (e.g., see [34]), sound waves, plasmas, etc., basically wherever the governing equations are the same or similar. One such example is the long-term evolution (from some initial far-from-equilibrium state) of 1D δ-interacting bosons, which is governed by a quantum integrable model [32,33] but is not yet fully understood (apart from the hard-core regime [27]).